Available online at www.sciencedirect.com
SCIENCE DIRECT®
Astroparticle Physics 20 (2003) 221–234
Astroparticle Physics
www.elsevier.com/locate/astropart

Atmospheric production of energetic protons, electrons and positrons observed in near Earth orbit

P. Zuccon [a,*], B. Bertucci [a], B. Alpat [a], G. Ambrosi [a], R. Battiston [a], G. Battistoni [b], W.J. Burger [a], D. Caraffini [a], C. Cecchi [a], L. Di Masso [a], N. Dinu [a], G. Esposito [a], A. Ferrari [b,c], E. Fiandrini [a], M. Ionica [a], R. Ionica [a], G. Lamanna [a,c], M. Menichelli [a], M. Pauluzzi [a], P.R. Sala [b,d]

[a] *Universitá and Sezione INFN of Perugia, I-06123 Perugia, Italy*
[b] *Sezione INFN of Milano, I-20133 Milano, Italy*
[c] *CERN, CH-1211 Geneva, Switzerland*
[d] *ETH, CH-8092 Zurich, Switzerland*

Received 19 March 2003; accepted 16 April 2003

Abstract

Substantial fluxes of protons and leptons with energies below the geomagnetic cutoff have been measured by the AMS experiment at altitudes of 350–390 km, in the latitude interval ±51.7°. The production mechanisms of the observed trapped fluxes are investigated in detail by means of the FLUKA Monte Carlo simulation code. All known processes involved in the interaction of the cosmic rays with the atmosphere (detailed descriptions of the magnetic field and the atmospheric density, as well as the electromagnetic and nuclear interaction processes) are included in the simulation. The results are presented and compared with experimental data, indicating good agreement with the observed fluxes. The impact of the secondary proton flux on particle production in atmosphere is briefly discussed.

1. Introduction

Cosmic rays approaching the Earth interact with the atmosphere resulting in a substantial flux of secondary particles. The knowledge of the composition, the intensity and the energy spectra of these particles is relevant, e.g. for the evaluation of background radiation for satellites experiments and manned spacecrafts and for the estimation of the atmospheric neutrino production for neutrino oscillation experiments [1–3].

Different approaches are used to model the production in atmosphere and the transport of charged particles in the magnetosphere. At low energies (KeV–MeV) the collective properties of the particles are described by means of diffusion and transport equations in a semi-quantitative way [4–10]. At higher energies, where the particle density is low, a single-particle approach is feasible using Monte Carlo methods for particle production and precise transport algorithms allow for an accurate description of the particle behavior.

* Corresponding author.
E-mail address: paolo.zuccon@pg.infn.it (P. Zuccon).

0927-6505/$ - see front matter © 2003 Elsevier B.V. All rights reserved.
doi:10.1016/S0927-6505(03)00160-9

The AMS measurements in near Earth orbit [11,13] provided the first accurate information on the intensity, energy spectra and geographical origin of charged particle fluxes at energies below the geomagnetic cutoff over a wide range of latitudes and longitudes. The under cutoff component of proton fluxes at equatorial latitudes has revealed an intensity up to 50% of the primary proton flux. A positron–electron flux ratio has been found in the under cutoff component which largely exceeds the corresponding cosmic rays ratio. Differences in residence times and geographical origins have been established for positively and negatively charged particles.

A robust interpretation of the characteristics of the under cutoff fluxes in terms of secondary particles produced in the atmosphere requires an accurate description of the interaction processes at their origin and the geomagnetic field effects. Interpretations of the AMS measurements have been proposed [14,15] based on Monte Carlo simulations using different approaches on both the generation technique and the interaction model.

In this work, we report results from a Monte Carlo simulation based on FLUKA 2000 [16] for the description of cosmic ray interactions with the atmosphere which uses a 3D description of both the interactions and the geometry of the Earth. The key features of our approach are the efficient generation technique for the incoming cosmic rays flux and a true microscopic, theory driven treatment of the interaction processes as opposed to empirical approaches used in the past.

In the following section we give a detailed description of the basic ingredients of our simulation, the generation technique and the interaction model. In Section 3 we present our results for protons and leptons, and the comparison with the AMS measurements.

2. The model

The flux reaching the Earth magnetosphere is composed of particles emitted from the Sun and galactic cosmic rays. In the energy range of the AMS measurements the solar particle contribution is negligible.

The isotropic flux of Hydrogen and Helium nuclei is uniformly generated on a geocentric spherical surface with a radius of 1.07 Earth radii ($\sim$500 km above sea level) in the kinetic energy range 0.1–800 GeV/nucleon.

The contribution of cosmic rays nuclei heavier than Helium has been neglected since the expected contribution ($\sim$7%) to the production of secondary particles is of the same order of the uncertainties in the knowledge of Hydrogen and of Helium primary fluxes.

The analytical functions describing the H and He fluxes are taken from Ref. [17], and correspond to the solar activity detected at the time of the AMS measurements (June 1998).

The magnetic field in the proximity of the Earth includes two components: the Earth's magnetic inner field, calculated using a 10 harmonics IGRF [18] implementation, and the external magnetic field, calculated using the Tsyganenko Model [1] [19]. To account for the geomagnetic effects, for each primary particle we backtrace the corresponding antiparticle of the same energy until one of the following conditions are satisfied:

(1) the particle reaches the distance of 10 R_E from the Earth's center.
(2) the particle touches again the production sphere.
(3) neither 1 or 2 is satisfied before a time limit is reached.

If condition 1 is satisfied the particle is on an allowed trajectory, while if condition 2 is satisfied the particle is on a forbidden one. Condition 3 arises for only a small fraction ($\sim 10^{-6}$) of the events.

Particles on allowed trajectories are propagated forward and can reach the Earth's atmosphere. The atmosphere around the Earth is simulated up to 120 km a.s.l. using 60 concentric layers of homogeneous density and chemical composition.

[1] The external magnetic field is calculated only for distances greater than 2 Earth's radii (R_E) from the Earth's center . Its contribution to the total magnetic field is <1% at smaller distances and therefore can be neglected.

Data on density and chemical composition are taken from the standard MSIS model [20]. Above 120 km the atmosphere density is so small that the probability for a particle to interact is negligible. The Earth is modelled as a solid sphere which absorbs each particle reaching its surface.

A detailed description of the setup of this simulation can be found in [26].

2.1. The generation technique

The ideal approach in the generation of the primary cosmic rays spectra would be to start with an isotropic distribution of particles at a great distance (typically 10 R_E) from the Earth where the geomagnetic field introduces negligible distortions on the interstellar flux at the energies relevant for this work. However, this computational method is clearly inefficient. Kinematic cuts applied in order to improve the generation efficiency tend to introduce a bias for the low rigidity particles.

A good alternative to this approach is a back-tracing method [14,21] adopted in the present analysis as outlined in the previous section. In the following, we discuss the validity of the technique and report the results of a comparison of the two methods. This method was applied for the first time for the generation of atmospheric neutrino fluxes [3].

Let us consider first the effects of the geomagnetic field on an incoming flux of cosmic charged particles in the absence of a solid Earth.

For the discussion, we start with an isotropic flux of monoenergetic [2] particles at large distance from the origin of a geocentric reference system. In this scenario, a small fraction of particles, with very particular initial kinematic parameters, will follow complicated paths and remains confined at a given distance from the origin (semi-bounded trajectories); for all practical purposes this sample can be neglected. Most of the particles will follow unbounded trajectories, reaching again infinity after being deflected by the magnetic field.

[2] The realistic case of an energy spectrum can be treated just as a superposition of monoenergetic cases.

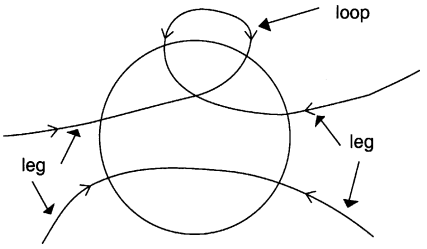

Fig. 1. Trajectories types crossing a spherical surface around the Earth.

Unbounded trajectories cross a spherical surface centered in the field source only an even number of times, as shown in Fig. 1: we call *legs* the trajectory parts connecting the spherical surface to infinity and *loops* the parts of the trajectory starting and ending on the spherical surface.

Since each trajectory can be followed in both directions and no source or sink of particles is contained within the surface, the incoming and outgoing fluxes are the same. However, the presence of the magnetic field breaks the isotropy of the flux "near" the field source, so for a given location there is a flux dependence due to the direction.

Applying the Liouville theorem, under the hypothesis of isotropy at infinity, it is straightforward to demonstrate [22] that the particles flux at an arbitrary point is the same as at infinity along a set of directions (allowed directions), and zero along all the others (forbidden directions).

The pattern of the allowed and forbidden directions depends on both the rigidity and the location and is known as the geomagnetic cutoff.

With the introduction of a solid Earth, all the trajectories that cross the Earth are broken in two or more pieces (Fig. 2): the legs become one-way trajectories and the loops disappear.

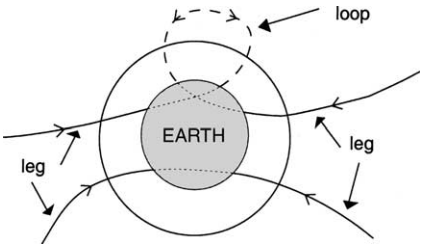

Fig. 2. Trajectories in the presence of a solid Earth.

The presence of the Earth modifies the flux which exits from the surrounding spherical surface, since particles are absorbed by the Earth, while it has only a minimal effect on the incoming flux which is modified only by the absence of certain loops. To generate the flux of particles reaching the Earth's atmosphere, it is sufficient to follow the particles along the allowed trajectories corresponding to the legs, taking care to avoid double or multiple counting.

To respect this prescription we reject all trajectories that are backtraced to the production sphere, this allow us to correctly consider the cases like the one shown in Fig. 3.

We point out that an important difference with respect to the application in the neutrino flux calculation of [3] is that for the latter, as a consequence of the one dimensional approach, there are no problems of double counting.

To check the validity of our technique we made a test comparing the results of the "ideal" generation technique at 10 R_E distance from the Earth's center with the backtracing technique used here.

Fig. 4 shows this comparison for several characteristic distributions, the agreement between the two methods is good.

2.2. The interaction model

A custom version of the software package FLUKA 2000 [16] has been used to transport the particles and describe their interactions with Earth's atmosphere.

FLUKA is a general purpose Monte Carlo code for the simulation of hadronic and electromagnetic interactions. It has been used in many applications, and it is continuously checked using the available data from low energy nuclear physics, high energy accelerator experiments and measurements of particle fluxes in the atmosphere [23].

In FLUKA hadronic interactions are treated in a theory-driven approach, the general phenomenology is obtained from a microscopical description of the interactions between the fundamental constituents (quarks and nucleons) appropriate for the different energy regions. Below an energy of few GeV, hadron–nucleon interaction models are based on resonance production and decay of particles (PEANUT Model [24]), for higher energy ranges the Dual Parton Model is used. The extension from hadron–nucleon to hadron–nucleus interactions is done in the framework of a generalized intra-nuclear cascade approach including the Gribov–Glauber[25] multi-collision mechanism for higher energies followed by equilibrium processes: evaporation, fission, Fermi break-up and γ de-excitation. The parameters of the models used in FLUKA are fixed by comparing expectations with the available data from experiments. The Helium interactions with different target nuclei are treated in the framework of the superposition model.

The FLUKA approach to the simulation of the interaction naturally allows for a tridimensional description of the electromagnetic and hadronic interactions, particularly relevant for the present application since the behavior of the secondary particles in the geomagnetic field depends strongly on the initial angle between the geomagnetic field and the particle momentum. The setup of this simulation is derived from [1].

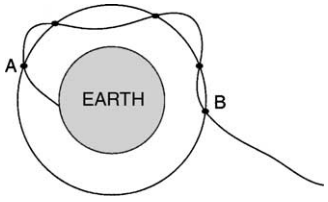

Fig. 3. An example of multiple counting along a trajectory, this type of trajectory has to be considered only at point B.

3. Comparison with the AMS data

To compare with the AMS data, we define a detection boundary placed at 400 km a.s.l. corresponding to a spherical surface matching the AMS orbit. We record each particle that crosses the detection boundary within the AMS field of view, defined as a cone with a 32° aperture [3] [11] with respect to the local zenith or nadir directions.

[3] For leptons the AMS field of view is reduced to a cone of 25° [13].

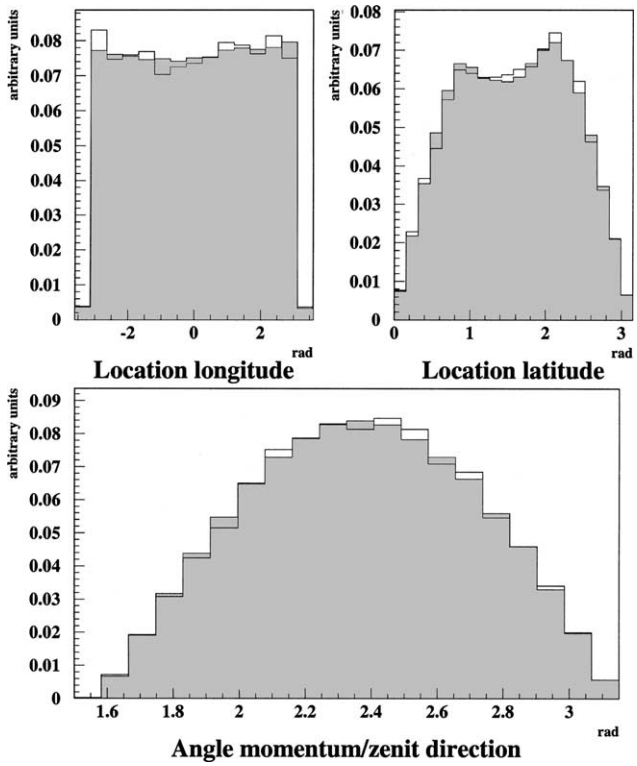

Fig. 4. Latitude and longitude of impact points and angle between momentum and zenith directions for particles generated at a distance of 10 Earth's radii (solid line) and particles generated with a backtracing technique at 1.07 Earth's radii (shaded histogram).

An absolute normalization of the simulated particle fluxes has been obtained calculating the equivalent time exposure (ETE) corresponding to the number of the generated primary cosmic rays [26].

The large surface of our detector ($\sim 4\times 10^{14}$ m^2) allows to collect a statistical sample comparable to the AMS data with an ETE of the order of 10^{-12} s.

Our results are based on a sample of $\sim 18.7\times 10^6$ primary protons generated in the kinetic energy range of 0.1–800 GeV, which corresponds to an ETE of 11.6×10^{-12} s and $\sim 3.1\times 10^6$ He nuclei on the kinetic energy range 0.1–800 GeV/nuc. corresponding to an ETE of 16.9×10^{-12} s.

3.1. Proton fluxes

Fig. 5 shows the comparison between the fluxes obtained with our simulation and the measured AMS down going, or zenith, proton flux [11] in nine intervals of geomagnetic latitude (θ_M) [27]. Fig. 6 shows the same comparison for the up going, or nadir, proton flux.

Different aspects of our simulation are involved in the description of the observed fluxes at energies above and below the geomagnetic cutoff. At energies above the geomagnetic cutoff, the generation technique and the global normalization can be tested independently from other aspects of the simulation. At energies below cutoff, all the aspects of this simulation are relevant.

The simulation reproduces well at all latitudes the high energy part of the spectrum and the falloff in the primary spectrum due to the geomagnetic cutoff, thus validating the general approach used for the generation and detection, as well as the tracing technique. Small fluctuations in the global agreement in the high energy part are consistent with the errors in the AMS data [12].

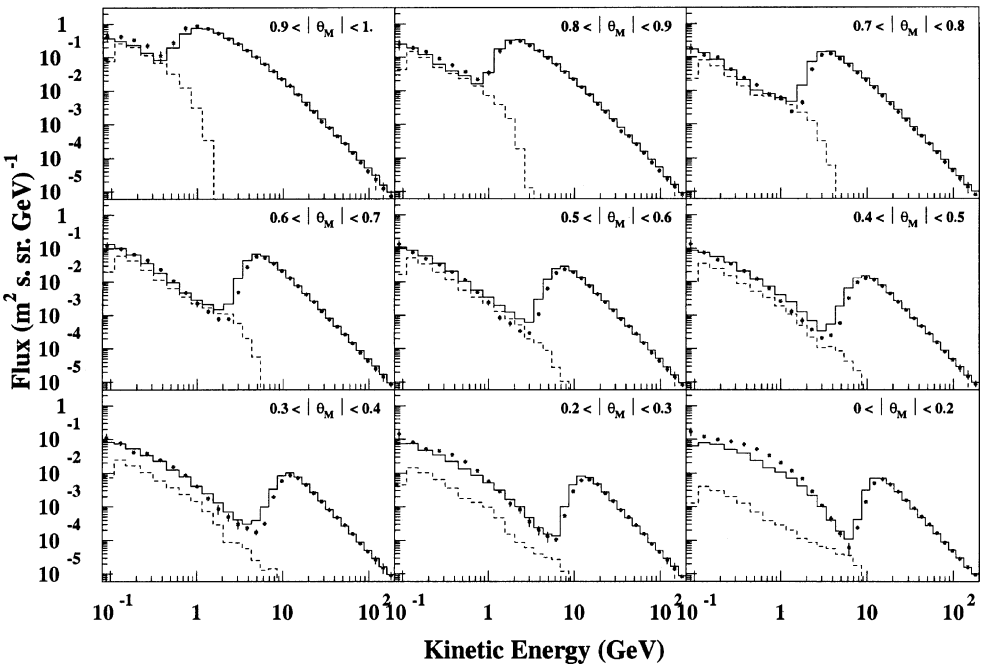

Fig. 5. Downgoing proton flux, simulation (solid line) and the AMS data (points); the dashed lines are described in the text. Θ_M is the geomagnetic latitude in radians. Errors in the simulated flux are of the same order as in the data.

In our simulation, only secondary protons produced in the interactions of the primary cosmic rays with the atmosphere are populating the under cutoff region of the spectrum. The comparison with the observed fluxes in this portion of the spectra is therefore relevant for an interpretation of the experimental data and to study the physical processes and the dynamical features at their origin. At the same time, any discrepancy arising in this comparison can be used to critically evaluate the limit of our approach.

For the under cutoff part of the spectrum we observe an underestimation of the flux at the level of 20% which can be expected from the approximations of the cosmic ray flux (missing contributions of heavier nuclei in the primary flux, uncertainties in the slope of the H and He spectra).

When compared with similar studies [14,15], this shows the best agreement with the AMS under cutoff data obtained so far.

The under cutoff flux is due to the secondaries, produced in the atmosphere, that spiral along the geomagnetic field lines up to the detection altitude. These particles represent only a tiny fraction of all secondaries produced in atmospheric interactions of cosmic rays (~7% of events), and correspond to protons generated under peculiar kinematical conditions in the early stages of the shower development. Fig. 7 shows that under cutoff protons are generated preferentially by cosmic rays grazing the atmosphere and interacting, on average, at higher altitudes (36.5 km) with respect to the full sample of the primary cosmic rays (25.2 km).

Using a classification based on the time interval between the production of a secondary particle and its subsequent re-absorption in the atmosphere (residence time), it is possible to distinguish two populations in the under cutoff particles [11]. Fig. 8 shows the residence time versus the kinetic energy of the under cutoff protons for AMS data [28] (left) and as obtained in our simulation (right). The line superimposed on the plots separates the *short lived* population, characterized by residence time below ~0.3 s, from the *long lived* one with residence times up to some tens of seconds.

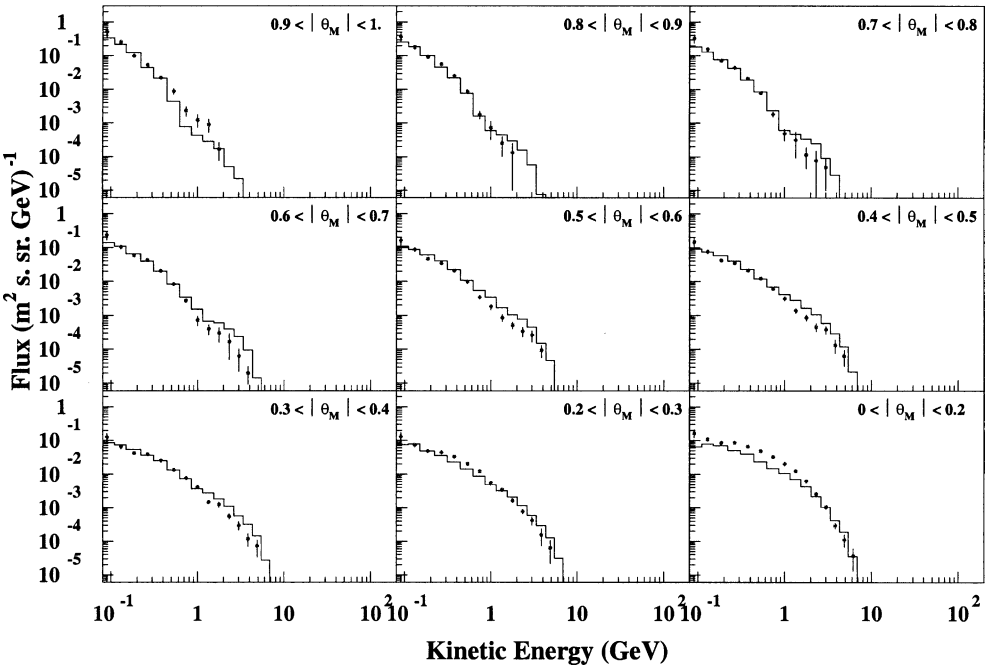

Fig. 6. Upgoing proton fluxes, simulation (solid line) and the AMS data (points).

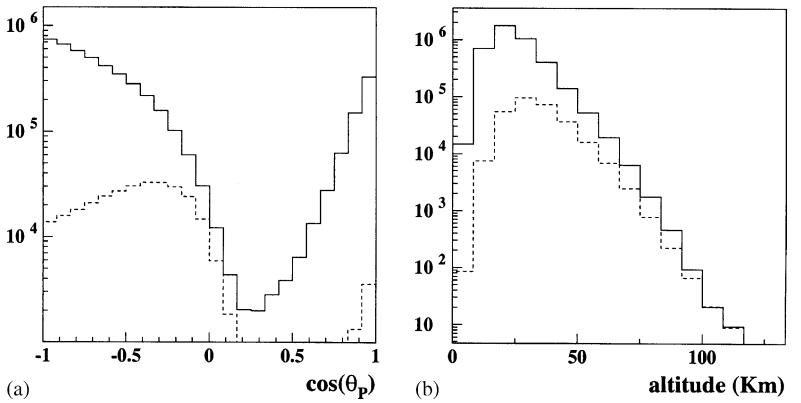

Fig. 7. (Left) The distribution of the zenith angle of the primary protons at the moment of the interaction in the atmosphere. (Right) The distribution of the altitude of the interaction of the primary cosmic rays with the atmosphere. Dashed lines represent the subsample of primary protons generating the secondary protons detected by AMS.

The presence of the two populations can be explained within the formalism of the adiabatic invariants [29], since trapped particles move along magnetic drift shells. The residence time of an under cutoff particle depends on the fraction of the shell located inside the Earth's atmosphere. Particles with short residence times move along shells (short lived) with large intersections with the Earth's atmosphere thus they can do only few bounces from the northern to the southern

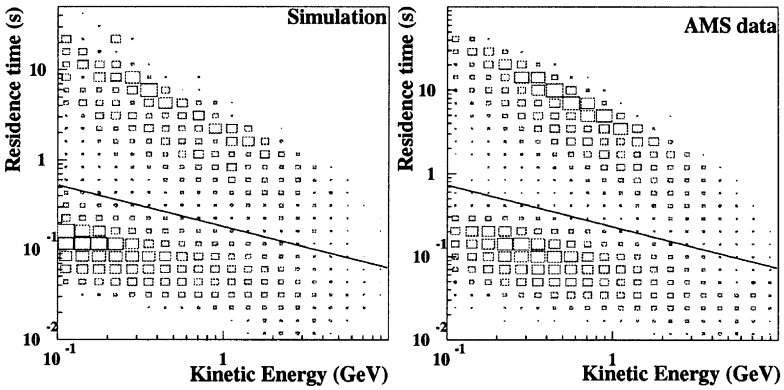

Fig. 8. Residence time versus kinetic energy for secondary protons produced in the interactions of primary cosmic rays with the atmosphere. The protons are detected at geomagnetic latitude $|\theta_M| < 0.7$ rad.

hemisphere before to re-interact on an atmospheric nucleus. Conversely particles with a long residence time move on shells (long lived) that intersect the atmosphere only in the South Atlantic Anomaly region, thus they can make a nearly complete revolution around the Earth before to re-

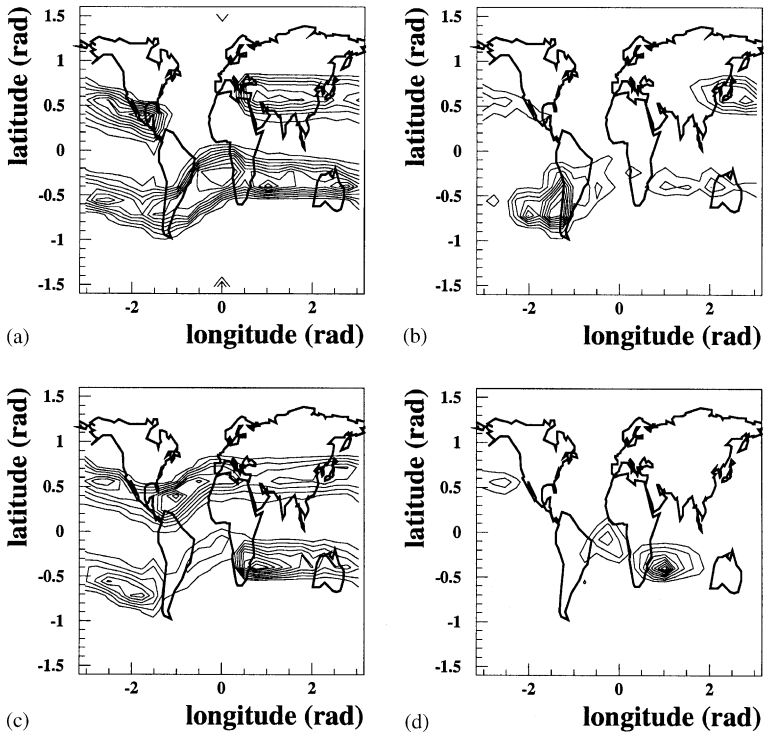

Fig. 9. Maps of secondary protons origin (upper plots) and reabsorption (lower plots) points detected at geomagnetic latitude $|\theta_M| < 0.7$ rad. Left plots are relative to the short lived population (residence time < 0.3 s), right plots are relative to the long lived population (residence time > 0.3 s).

interact with the atmosphere. This is confirmed in Fig. 9 which shows the generation and the absorption points of the under cutoff particles in the atmosphere separately for particles with long and short residence times. Most of the drift shells crossed by AMS orbit, at an altitude of 400 km, are short lived, the contribution of long lived shells is practically negligible in the polar region, and become more and more important as one approaches the equatorial region [30].

Particles moving along long lived shells have a large probability to cross many times a geocentered spherical detector, while those moving along short lived shells typically cross the detector only once or twice. This simulation permits to distinguish the flux of secondary particles that re-interacts at every instant with the atmosphere, *interacting flux*, from the flux circulating in the near Earth orbit. The two fluxes differ because of the presence of long lived particles which circulates around the Earth for times up to some tens of seconds. The dashed lines in Fig. 5 represent the interacting flux, obtained in our simulation counting only once each particle that crosses our geocentered spherical detector. As expected the difference between the solid and the dashed lines is evident in the equatorial region where the contribution of long lived particles is important and tends to vanish as approaching to the polar region.

Fig. 10 better shows this effect as a function of the geomagnetic latitude: the intensity of the interacting flux and that of the measured one are compared with the integral of the primary flux. The interacting flux is nearly one order of magnitude smaller than the primary one at all the latitudes, therefore only a minor contribution from the under cutoff proton component is expected in the atmospheric shower development and in particular for the atmospheric neutrino production.

3.2. Electrons and positrons

Fig. 11 shows the positron and electron fluxes, measured by AMS (points) compared with the results of our simulation (solid lines). The fluxes corresponds to the zenith attitude of AMS and are subdivided in six intervals of geomagnetic latitude as in [13]. Since cosmic fluxes of $e^{\pm}$ are not included in our simulation, the comparison is relevant only for the under cutoff part of the spectrum.

A good agreement is observed for both positrons and electrons at $|\theta_M| < 0.9$.

At higher latitudes, the simulated $e^{\pm}$ fluxes are definitely lower than the AMS observations, whereas for protons only a minor deficit was observed. This is justified by the missing contribution of cosmic $e^{\pm}$ fluxes, which are neglected in our simulation, but become relevant at low energies for the polar latitudes.

Only 3.4% of the primary cosmic rays reaching the Earth atmosphere produce e^- and e^+ detectable by AMS at 400 km. These $e^{\pm}$ are produced in preference by primary cosmic rays grazing the atmosphere, as in the case of the under cutoff protons.

Electrons and positrons are produced mostly by the decays of charged and neutral pions. Charged pions contribute to electrons and positrons populations, through the chain:

$$\pi^{\pm} \to \mu^{\pm} \to e^{\pm} \tag{1}$$

while neutral pions produce equivalent amounts of e^- and e^+ through the chain:

$$\pi^0 \to \gamma\gamma \to 2(e^+ + e^-) \tag{2}$$

The relative contributions of charged and neutral pions to the under cutoff flux of e^- and e^+ observed in AMS depend on the combination of two factors: the features of the primary CR interaction (i.e. multiplicity and energy of charged/neutral pions, Table 1) and the charge dependent transport of the secondaries in the geomagnetic field.

Table 1 shows, at four typical energies, the mean multiplicity and the mean energy fraction of protons and pions produced in the interaction of the cosmic rays with the atmosphere. The relative abundance of charged and neutral pions is energy dependent: at low energies the production of π^+ is favored as a consequence of the initial charge bias, at higher energies the charge asymmetry tends to vanish and the π^0 contribution becomes the most important.

Fig. 12 shows the relative contribution of the different charge states of the pions to the

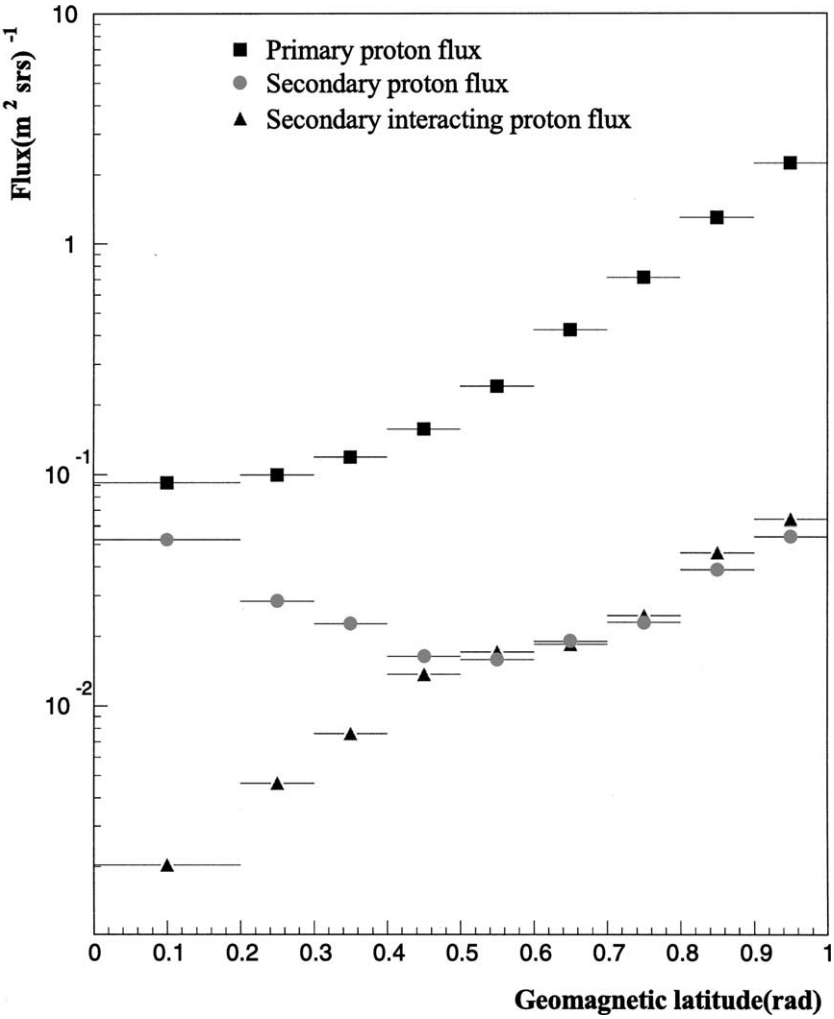

Fig. 10. Energy integrated primary proton flux as function of the geomagnetic latitude, compared to the secondary proton flux and to the *interacting proton* flux, see text for more detail.

production of under cutoff e^- and e^+ as a function of their detection geomagnetic latitude. The π^0 relative contribution increases with latitude, representing a $\sim$55% (60%) of the $e^{+(-)}$ flux source at $|\theta_M| > 0.5$. This is expected from the generated multiplicities of neutral/charged pions in the proton interactions with the atmosphere (Table 1). Geomagnetic effects are responsible for the large enhancement of the charged pion contribution observed for e^- and e^+ at lower geomagnetic latitudes.

Fig. 13 shows, as a function of the geomagnetic latitude, the fraction of eastward [4] going primary protons responsible for secondary protons (filled squares), positrons (open circles) and electrons (empty squares) observed in our AMS-like detector. A clear dominance of eastward going pro-

[4] East–West direction is defined with respect the local B field. Local magnetic azimuthal angle convention is the one adopted in [31].

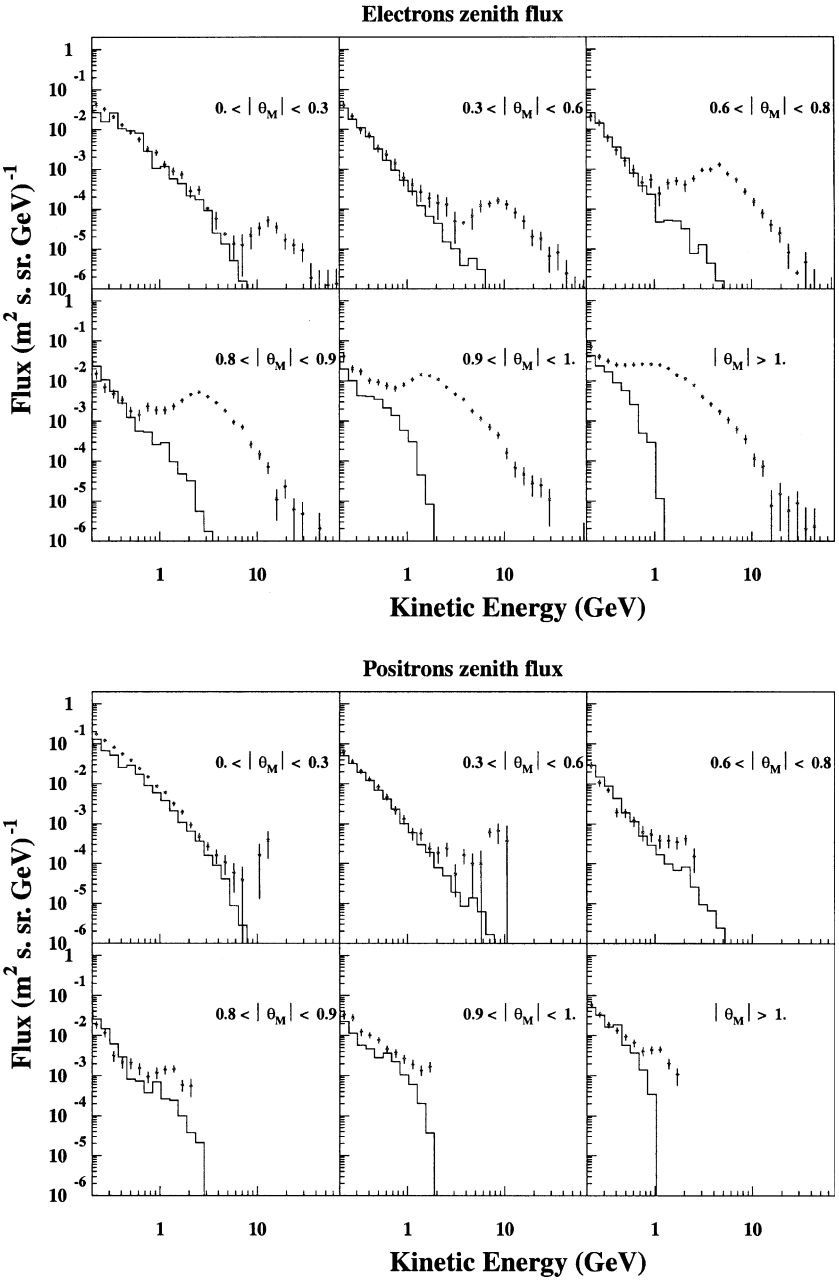

Fig. 11. Downgoing positron and electron fluxes in six regions of geomagnetic latitude θ_M, solid histogram (simulation) points (AMS data).

tons is observed for the production of positive charged secondaries (protons and positrons) at low geomagnetic latitudes. The effect is reduced with increasing latitudes and tends to vanish in the polar region. The opposite trend is found for the protons producing electrons. The underlying mechanism has been suggested for the first time in [21]: protons grazing the atmosphere going

Table 1
Energy fraction and multiplicity of secondary particles produced in the proton interactions with atmospheric nuclei in FLUKA 2000

Particle	5 GeV		10 GeV		20 GeV		30 GeV	
	Mult.	E frac.	Mult.	E frac.	Mult.	E frac.	Mult.	E frac.
p	1.983	0.409	2.676	0.337	2.744	0.307	2.770	0.294
π^+	0.711	0.131	1.292	0.149	1.970	0.159	2.381	0.164
π^-	0.389	0.068	0.975	0.098	1.641	0.116	2.047	0.122
π^0	0.638	0.114	1.601	0.169	2.378	0.175	2.840	0.177

Four typical energies of primary protons are considered.

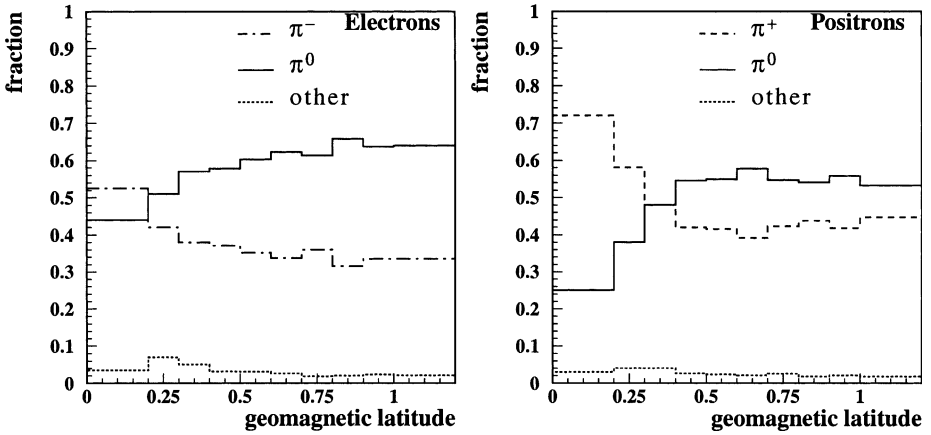

Fig. 12. Relative contribution of the charged and neutral pions to the under cutoff lepton fluxes observed by AMS at 400 km a.s.l., expressed as function of the geomagnetic latitude.

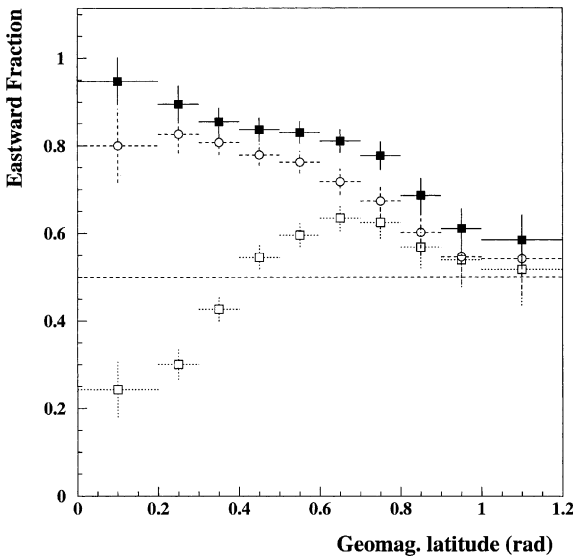

Fig. 13. Fraction of secondary particles generated by eastward going primaries as function of the geomagnetic latitude. Filled squares protons, open circles positrons, open squares electrons.

towards East (West) are expected to favor the production of upward moving positrons (electrons) which can therefore escape atmosphere. The opposite is true if the charge sign of secondaries is reversed.

This effect, combined with the East–West asymmetry of the rigidity cutoff for primaries, has a relevant influence on the different spectra for e^- and e^+ escaping the atmosphere after generation. Fig. 14 shows the ratio of under cutoff positron and electron fluxes as a function of geomagnetic latitude measured by AMS (black squares) and in our simulation (open circles). The peculiar dependence of this ratio with latitude and in particular the net positron dominance at $|\theta_M| < 0.5$ are well reproduced in our simulation. It is clear from our simulation that this behavior is mostly due to geomagnetic effects, and cannot be attributed to charge asymmetry at production (Table 1 and Fig. 14). The positron dominance near the equator is

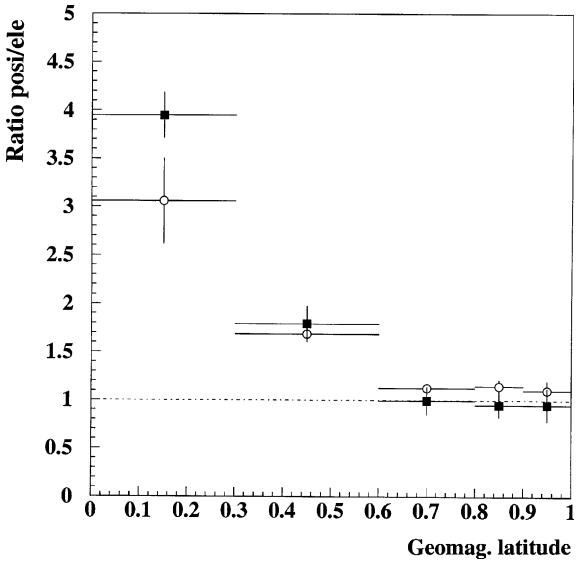

Fig. 14. The ratio of the under cutoff positron and electron fluxes, as function of geomagnetic latitude. Open circles (this simulation), filled squares (AMS data).

due to the lower geomagnetic cutoff experienced by eastward going primaries, which are preferably injecting positrons at the AMS altitude. The positron dominance tends to vanish going towards magnetic poles, as the East–West asymmetry effect reduces.

4. Conclusions

The interactions of cosmic rays with the Earth's atmosphere and magnetosphere have been investigated by means of a fully 3D Monte Carlo based on the FLUKA package. The AMS measurements of under cutoff protons, electrons and positron fluxes in near Earth orbit have been used to assess the quality of our simulation.

A detailed analysis of the possible strategies for the generation of the incoming cosmic ray flux has demonstrated the validity of the backtracing approach as a reliable and efficient technique. The role of geomagnetic effects in the charge composition and the dynamical features of the under cutoff fluxes has been studied in detail. The East–West asymmetry in the rigidity cutoff, associated to a charge sign dependent efficiency in the transport of secondaries at the AMS altitude, has been confirmed at the origin of the excess of the positron component in the under cutoff spectra. The geographical origin and the residence time distributions for both protons and leptons have been reproduced and the effect of the presence of a long-lived component has been discussed.

The experimental flux intensities, as well as their peculiar kinematical features, have been reproduced in our simulation at the ~20% level. This can be taken as a strong indication that the main source of radiation in the near Earth region—at least outside the region of the South Atlantic Anomaly—is the interaction of the primary cosmic rays with the atmosphere. Our results indicate the flux intensity of this under cutoff radiation re-interacting with the atmosphere (interacting flux) never exceeds a 10% of the cosmic proton flux, thus representing a minor source for atmospheric production of secondaries.

In our simulation, a truly microscopical description of the particle interaction is used for the first time in conjunction to a fully 3D geometry setup and an efficient generation technique. After its successfull validation with the AMS data, we believe that this represents a valuable tool to assess the radiation environment in near Earth orbit and to perform accurate calculation of particle fluxes in the atmosphere.

Acknowledgement

This work has been partially supported by the Italian Space Agency (ASI) under contract ASI I/R/211/00.

References

[1] G. Battistoni, A. Ferrari, T. Montaruli, P.R. Sala, The FLUKA atmospheric neutrino flux calculation, hep-ph/0207035;
G. Battistoni et al., A 3-dimensional calculation of the atmospheric neutrino fluxes, Astropart. Phys. 12 (2000) 315.
[2] G. Barr et al., Phys. Rev. D 39 (1989) 3532;
V. Agrawal, T.K. Gaisser, P. Lipari, T. Stanev, Phys. Rev. D 53 (1996) 1314.
[3] M. Honda et al., Calculation of the flux of atmospheric neutrinos, Phys. Rev. D 52 (1995) 4985.

[4] S.B. Treiman, The cosmic ray albedo, Phys. Rev. 91 (1953) 957.
[5] E.C. Ray, Reentrant cosmic ray albedo calculation, J. Geophys. Res. 67 (1962) 3289.
[6] P.J. Konig et al., A model for the anysotropic reentry of albedo, J. Geophys. Res. 86 (1981) 515.
[7] N.L. Grigorov, Akademia Nauk, SSSR, Doklady, 234 (1977) 810.
[8] S.D. Verma, A calculation of the flux and energy spectrum of secondary electrons at the high altitudes in the atmosphere, Proceedings of the Indian Academy of Sciences A 56 (1967) 125.
[9] A.A. Gusev et al., Formation of albedo electron fluxes in the geomagnetic field, Geomagn. Aeronomy 22 (6) (1982) 754.
[10] Boscher et al., Dynamic model of high energy proton belt, in: Proceedings of the ESA Workshop on Space Weather, The Nederlands, 1998.
[11] AMS Collaboration, J. Alcaraz et al., Protons in near Earth orbit, Phys. Lett. B 472 (2000) 215.
[12] AMS Collaboration, J. Alcaraz et al., Cosmic protons, Phys. Lett. B 490 (2000) 27.
[13] AMS Collaboration, J. Alcaraz et al., Leptons in near Earth orbit, Phys. Lett. B 484 (2000) 10.
[14] L. Derome et al., Origin of the high-energy proton component below the geomagnetic cutoff in near Earth orbit, Phys. Lett. B 489 (2000) 1;
L. Derome et al., Secondary electrons and positrons in near earth orbit, Phys. Lett. B 515 (2001) 1.
[15] V. Plyaskin, Calculation of atmospheric neutrino flux, Phys. Lett. B 516 (2001) 213.
[16] A. Fasso, A. Ferrari, P.R. Sala, Electron–photon transport in FLUKA: status, in: A. Kling, F. Barao, M. Nakagawa, L. Tavora, P. Vaz (Eds.), Proceedings of the MonteCarlo 2000 Conference, Lisbon, October 23–26, 2000, Springer-Verlag, Berlin, 2001, pp. 159–164;
A. Fasso, A. Ferrari, J. Ranft, P.R. Sala, FLUKA: status and prospective for hadronic applications, in: A. Kling, F. Barao, M. Nakagawa, L. Tavora, P. Vaz (Eds.), Proceedings of the MonteCarlo 2000 Conference, Lisbon, October 23–26 2000, Springer-Verlag, Berlin, 2001, pp. 955–960.
[17] T.K. Gaisser, M. Honda, P. Lipari, T. Stanev, Primary spectrum to 1 TeV and beyond, in: Proceedings of the 27th ICRC (Hamburg, 2001), Session OG1.01.
[18] N.A. Tsyganenko, Geomagn. Aeronomy (1986) 523;
N.A. Tsyganenko, M. Peredo, Geopack Manual, (1992).
[19] N.A. Tsyganenko, D.P. Stern, A new-generation global magnetosphere field model, based on spacecraft magnetometer data, ISTP Newslett. 6 (1996) 21.
[20] A.E. Hedin, Extension of the MSIS thermospheric model into the middle and lower atmosphere, J. Geophys. Res. 96 (1991) 1151.
[21] P. Lipari, The fluxes of subcutoff particles detected by AMS, the cosmic ray albedo and atmospheric neutrinos, Astropart. Phys. 16 (2002) 295.
[22] M.S. Vallarta, Theory of the geomagnetic effects of cosmic radiation, in: Encyclopedia Handbuch der Physik, XLVI/1, Springer, 1961, p. 88.
[23] A. Ferrari, P.R. Sala, The physics of high energy reactions, in: A. Gandini, G. Reffo (Eds.), Proceedings Workshop on Nuclear Reaction Data and Nuclear Reactors Physics, Design and Safety, ICTP Miramare–Trieste (Italy) May 1996, World Scientific, 1998, p. 424.
[24] A. Ferrari, P.R. Sala, Intermediate and high energy models in FLUKA: improvements, benchmarks and applications, in: G. Reffo, A. Ventura, C. Grandi (Eds.), NDST-97, Trieste (Italy), May 19–24 1997, Proceedings of the International Conference on Nuclear Data for Science and Technology, Vol. 59, Part I, Italian Phys. Soc., Bologna, 1997, p. 247.
[25] R.J. Glauber, G. Matthiae, High-energy scattering of protons by nuclei, Nucl. Phys. B 21 (1970) 135.
[26] P. Zuccon, A Monte Carlo description of the cosmic rays interaction with the near Earth environment, Ph.D. Thesis, Perugia (Italy), 2002, http://ams.pg.infn.it/Tesi/tesi_zuccon.pdf.
[27] G. Gustaffson et al., J. Atmos. Terr. Phys. 54 (1992) 1609.
[28] G. Esposito, Study of cosmic ray fluxes on low Earth orbit observed with the AMS experiment, Ph.D. Thesis, Perugia 2002 http://ams.pg.infn.it/Tesi/tesi_esposito.pdf.
[29] C.E. Mc Illwain, J. Geophys. Res. 66 (1961) 1151.
[30] E. Fiandrini et al., Leptons with $E > 200$ MeV trapped in the Earth's radiation belts, J. Geophys. Res. 107A6 (2002).
[31] Kruglanski et al., Improvement of the trapped proton anisotropy description, TREND3 Tech. Note N. 6/2 (1998) 7–10.